

Synthesis and characterization of a magnetic hybrid catalyst containing lipase and palladium and its application on the dynamic kinetic resolution of amines

Clara A. Ferraz^a, Marcelo A. do Nascimento^b, Rhudson F.O. Almeida^b, Gabriella G. Sergio^a, Aldo A.T. Junior^a, Gisele Dalmônico^c, Richard Caraballo^c, Priscilla V. Finotelli^c, Raquel A.C. Leão^{b,d}, Robert Wojcieszak^e, Rodrigo O.M.A. de Souza^d, Ivaldo Itabaiana Jr.^{a,e,*}

^a Department of Biochemical Engineering, School of Chemistry, Federal University of Rio de Janeiro, 21941-910, Brazil

^b BOSSGroup—Biocatalysis and Organic Synthesis Group, Chemistry Institute, Federal University of Rio de Janeiro, 21941-909, Brazil

^c CBPF, Brazilian Center of Physical Research, Rio de Janeiro, RJ, 22290-180, Brazil

^d Pharmacy School, Federal University of Rio de Janeiro, Rio de Janeiro, 21941-170, Brazil

^e Univ. Lille, CNRS, Centrale Lille, ENSCL, Univ. Artois, UMR 8181-UCCS-Unité de Catalyse et Chimie Du Solide, F-59000, Lille, France

ARTICLE INFO

Keywords:

Lipases
Hybrid catalysts
Chiral amines
Dynamic kinetic resolution
Nanoparticles

ABSTRACT

Recent papers estimates that about 40 % of drugs present chiral amines in their structure and their synthesis in a sustainable and cost-competitive way is still a challenge for the industry. Kinetic resolution is one of the most applied method to produce these desired compounds where the association with lipase as a catalyst is a good alternative. However, the use of separate racemization catalyst and enzymes in the reaction medium still limits recovery, recycling and can occasionally be responsible for decreasing in selectivity for the desired product. In this work we proposed the synthesis and characterization of a hybrid magnetic catalyst composed containing lipase CaL B and Pd immobilized on the same recovered nanometric magnetic support for the application on Dynamic Kinetic Resolution of (*rac*)-1-phenylethylamine both in batch and continuous flow conditions. As results it was possible to achieve 99 % of conversion, with 95 % of selectivity and 93 % of enantiomeric excess after 12 h in batch. For a continuous flow system, it was possible to achieve 95 % of conversion with 71 % of selectivity and *ee* > 99 % after 60 min of reaction. The hybrid catalyst had around 50–100 nm with nanoparticulated Pd (5–10 nm) on its surface, presented a superparamagnetic behavior without remaining magnetization and 22 emu/g of saturation magnetization.

Introduction

Enantiomerically pure amines have been playing an important role in the synthesis of building blocks for the pharmaceutical and agrochemical industries, being an important segment of the chiral molecule market [1]. Among the different production routes for these molecules, the kinetic resolution is still the most widely used method industrially [2].

In the context of green chemistry and new environmental restrictions being applied in several countries [3], the use of enzyme catalysts has many advantages, like the mild reaction conditions, and their good chemo, regio- and stereoselectivity [4]. Among the enzymes used in organic synthesis, lipase (triacylglycerol acylhydrolases, (E.C. 3.1.1.3)) has gained great importance in the last years, since it does not require

the use of cofactors, it has high specificity to substrates, good stability in organic media and it is able to catalyze a number of reactions with great selectivity [5].

In an enzymatic kinetic resolution, lipase reacts with both enantiomers at different rates arriving at optimal conditions in a maximum theoretical yield of 50 % [6]. In order increase this yield and convert the unreacted enantiomer, a racemization is performed, usually through a metal catalyst, generating a dynamic kinetic resolution (DKR). The combination of enzymatic resolution and metal racemization in a one-pot reaction increases the efficiency of the process, reduces costs, time and labor effort [7].

Even though some lipase-catalyzed DKR may be considered well established, the development of catalytic systems for the DKR of amines continues to attract great attention, and several papers were published

* Corresponding author.

E-mail address: ivaldo@eq.ufrj.br (I. Itabaiana).

<https://doi.org/10.1016/j.mcat.2020.111106>

Received 25 March 2020; Received in revised form 22 June 2020; Accepted 28 June 2020

2468-8231/ © 2020 Elsevier B.V. All rights reserved.

recently on this topic [2,6,8]. However, the construction of a robust DKR system is not easy, once some criteria should be taken into account: (i) the KR must display a sufficient enantioselectivity ($E\text{-value} = k_{\text{fast}}/k_{\text{slow}} \geq 20$), (ii) the enzyme and the racemization catalyst must be compatible with one another, (iii) the rate of racemization (k_{rac}) must be at least ten times faster than the enzyme catalyzed reaction of the slow reacting enantiomers (k_{slow}), and (iv) the racemization catalyst must not react with the product formed from the resolution. Among these requirements, the compatibility between the enzyme and racemization catalyst is generally the critical issue, since these catalysts often operate optimally under very different condition [9].

A new catalytic approach developed by our group [8] and by a few others [9,10] involves the co-immobilization of a metal and an enzyme in one single support. These hybrid catalysts allow cascade reactions to occur with an increased efficiency, since enzyme and metal are able to work in cooperation.

Once the catalytic reaction is conducted, the possibility to recycle biocatalysts is also determinant for the success of enzyme applications in industry [11]. Furthermore, in the pharmaceutical industry for example, it is essential to remove any traces of catalyst which may interfere in subsequent reactions and contaminate the final product [12]. The application of a magnetic field is an efficient way to separate and recover a catalyst and it has several advantages compared to other traditional techniques, since it is highly selective, it reduces the use of consumables and solvents, and it minimizes mass loss, since the separation can be done without removing the material from the reaction medium [13,14]. Several magnetic supports have already been developed for the immobilization of enzymes [15,16], however, to the best of our knowledge, this is the first time that a magnetic nanoparticle is used as support for a hybrid catalyst.

In the present work, we synthesized and characterized a hybrid super magnetic biocatalyst containing the lipase B from *Candida antarctica* (CALB) immobilized and reduced in situ palladium adsorbed and its application in the DKR of (*rac*)-1-phenylethylamine both under batch and continuous flow reactors as well as their comparisons with the commercial lipase Novozym 435 (N435) and palladium immobilized on barium sulfate.

Results and discussion

Synthesis and characterization of the magnetic support with palladium

The magnetic nanoparticles (MN) were synthesized using the Fe^{2+} and Fe^{3+} ions co-precipitation method. In order to obtain small and well dispersed nanoparticles, sonication steps and surface coating with oleic acid were also necessary. After covering and functionalization steps, it was investigated different concentrations of adsorbed palladium (MN@3%Pd, MN@4.5%Pd and MN@6%Pd, respectively) in the efficiency of the racemization of (*S*)-phenylethylamine. Aiming to evaluate conversion, enantiomeric excess and selectivity, a kinetic study was performed until 3 h of reaction. The results are shown in Fig. 1.

It is important to note that a robust hybrid catalyst is the one that converts 50 % of the starting enantiomer with 100 % of selectivity with the lowest enantiomeric excess value possible. This step is important, since some amine oxidation products in addition to the corresponding imine can be formed, reducing the selectivity of the reaction. On racemization assay, the MN@4.5%Pd showed 56 % of conversion of (*S*)-phenylethylamine with 96 % of selectivity and 4% of enantiomeric excess after 60 min. Although the selectivity of this catalyst was slightly less than that presented by MN@6% Pd, it was chosen for the next steps since the concentration of 3% Pd was not as efficient. The 4.5 % of Pd concentration may also have shown a good distribution of metal on the catalyst surface, generating a contact surface favorable to the reaction.

Xu and colleagues recently reported the increasing on Pd nanoparticles concentration from 1.5 % to 3 % inside cages of MIL-101 did

not improve the catalytic efficiency in the racemization of 1-phenylethylamine [2]. In this work, the best racemization results (46 % conversion, 76 % selectivity and 15 % enantiomeric excess) were achieved after 18 h. According to Shakeri et al., the relation between size and amount of Pd is not properly a role and should be evaluated in each system [17]. In this work total racemization of 1-phenylethylamine was achieved with 96 % of selectivity after 4 h with 3 % palladium supported on mesocellular foam. Our group also tested different commercial palladium catalysts and obtained the best results after 2.5 h with commercially available palladium supported on barium sulphate (96 % selectivity and 3 % enantiomeric excess) [18]. The previous work of Bäckvall's group reported a production of a hybrid catalyst in which CALB and nanopalladium species were co-immobilized into the compartments of mesoporous silica, where 1 % of enantiomeric excess after 4 h of reaction was achieved on racemization of 1-phenylethylamine. Recently, the group of Li et al. applied protein-polymer nanoconjugates as confined nanoreactors for the in situ synthesis of lipase-palladium (Pd) nanohybrids. The 0.8 nm Pd nanoparticles exhibited increased activity in racemization of (*S*)-1-phenylethylamine at 55 °C, that was more than 50 times that of commercial Pd/C. In the dynamic kinetic resolutions of pharmaceutical intermediates (\pm)-1-phenylethylamine, the lipase-Pd nanohybrids displayed 7.6 times higher efficiencies than the combination of N435 and Pd/C [10]. These results reaffirm the robustness of the data obtained by our catalyst.

The next steps in the construction of the hybrid catalyst starting from MN@4.5%Pd were accompanied by evaluation of its structure, morphology and magnetic properties. Through transmission electron microscopy (Fig. 2), the MN synthesized showed around 10–20 nm and non-uniform rounded shape (Fig. 2a). After coating with TEOS (Fig. 2b), it was still possible to confirm silica recovery of magnetic nuclei, achieving around 50 nm of diameter. Once Pd nanoparticles were produced in situ and adsorbed into surface, the deposition of medium diameter metallic particles ranging from 5–10 nm could be confirmed as shown in Fig. 2c that is in agreement with previous reported palladium catalysts supported on silica [2,19,20].

The presence of Pd on surface and the magnetic nuclei were confirmed by energy-dispersive X-ray spectroscopy as shown in Fig. 3. Iron and silicon (red and blue, respectively) were evenly distributed in the nanoparticles, and Pd (green) remained present only at some spots.

X-ray diffraction assays were also performed to evaluate iron oxide crystal's phase, the crystallinity and verify nanoparticles sizes (Fig. 4).

The peaks obtained in the MN diffractogram are in accordance to those already expressed in previous works and are characteristic of magnetite and maghemite crystals being a transitory phase between each other [21,22]. This transitory phase between crystal was already reported by other research groups on co-precipitation method [23,24] (Table 1).

The amorphous phase in the MN with TEOS and MN@4.5%Pd diffractograms are typical of amorphous silica coating. Besides the new wide peak in 40° in the MN@4.5%Pd is characteristic of non-valent palladium in a cubic face centered structure [25]. Through Scherrer's equation, the estimated crystallite size for iron oxide nanoparticles was 9 nm and for palladium nanoparticles was 3 nm.

The relation between the magnetization (*M*) and the applied field (*H*) on MN and MN@4.5%Pd showed in Fig. 5 confirmed the superparamagnetic properties of the nanoparticles, since the curves does not present hysteresis loops or magnetization remaining after field removal [26]. The saturation magnetization was around 60 emu/g and 22 emu/g for MN and MN@4.5%Pd, respectively [27]. These findings are even more interesting when it is taken into account that catalyst MN@4.5% Pd, even coated with mesoporous silica maintains its paramagnetic potential.

Immobilization of lipase CALB in the MN@4.5%Pd support

The immobilization efficiency of CALB on MN@4.5%Pd support

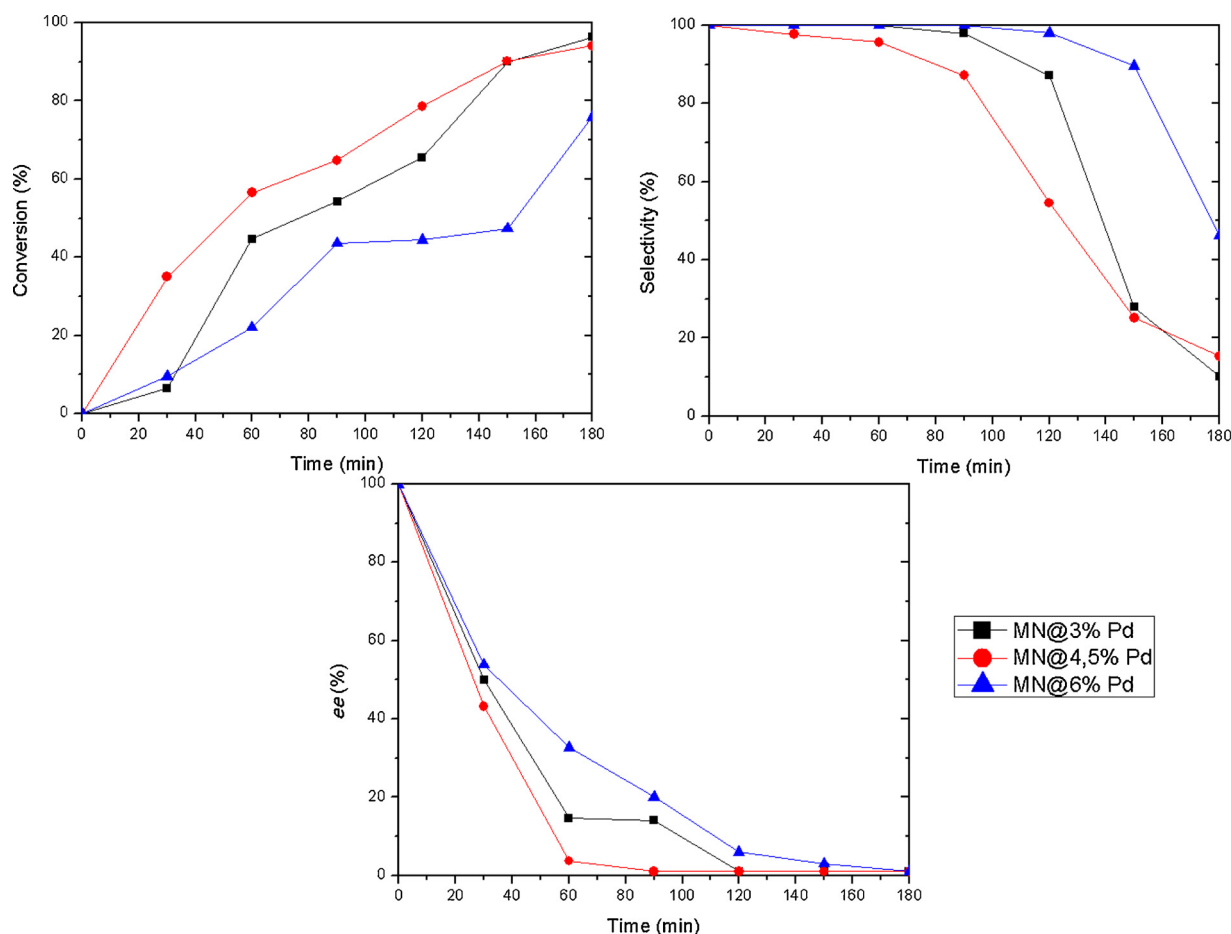


Fig. 1. Conversion, selectivity and ee of MN with palladium in the racemization reaction. * MN@3% Pd, MN@4.5% Pd and MN@6% Pd, = Magnetic nanoparticles with 3, 4.5 and 6 % of palladium, respectively.

with both glutaraldehyde (GLU) and epichlorohydrin (EPI) links was evaluated by Bradford method [28]. The FT-IR spectra (Fig. 6) of both immobilized biocatalysts were similar and evidences the presence of peptide bonds when compared to the support without (MN@4.5%Pd). The band at 1640 cm^{-1} corresponds to the axial vibration typical of secondary amide binding ($\text{CO}=\text{N}-\text{H}$), evidencing enzyme immobilization [27,29].

The new hybrid biocatalysts were investigated for hydrolytic activity, esterification potential as well as their application on in the DKR of (*rac*)-1-phenylethylamine. Table 2 compares the results for hydrolytic activity and esterification conversion after 1 h, 3 h and 6 h in comparison to commercial N435.

As observed, the hydrolytic activities showed by the new hybrid catalyst were substantially lower than MN@ catalyst. Lipase CALB is known to have limited hydrolysis activity of triacylglycerols. In addition, hybrid catalysts have a larger area filled with adsorbed Pd, which may have limited the functionalization step and subsequent

immobilization reaction. Comparing the esterification conversions through the time, the hybrid catalyst with GLU achieved superior higher results when compared with EPI and commercial N435 after 3 h and 6 h of reaction. Enzymatic immobilization can slightly modify enzymes' structures, which changes its activity depending on the reaction [30]. Rodrigues et al. compared the hydrolytic activity of chitosan support activated with both GLU and EPI in the immobilization of CALB. It was found that enzyme immobilized with GLU showed higher activity [31]. It was also verified that chitosan derivatives showed higher hydrophobicity, which is important for immobilization. The hybrid catalyst with GLU (MN@4.5%PdCALB) was chosen for the next steps.

Dynamic kinetic resolution of (*rac*)-1-phenylethylamine in batch conditions

The selected hybrid catalyst was submitted to optimization of the amount of immobilized enzyme, in order to evaluate the influence of

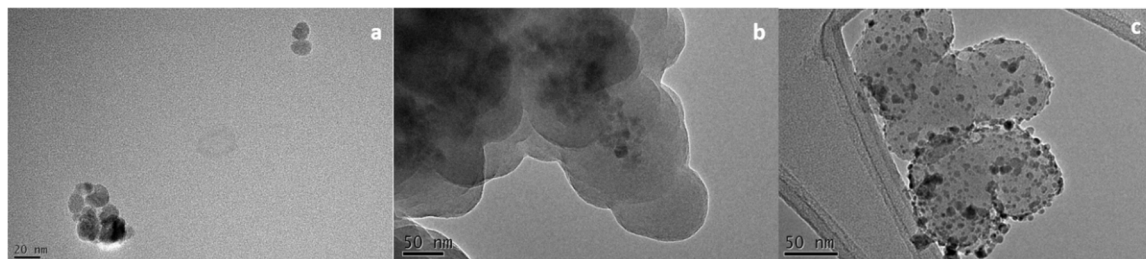


Fig. 2. Transmission electron microscopy of the MN@4.5%Pd. (a) MN synthesized through the co-precipitation method. (b) coating with TEOS and (c) palladium.

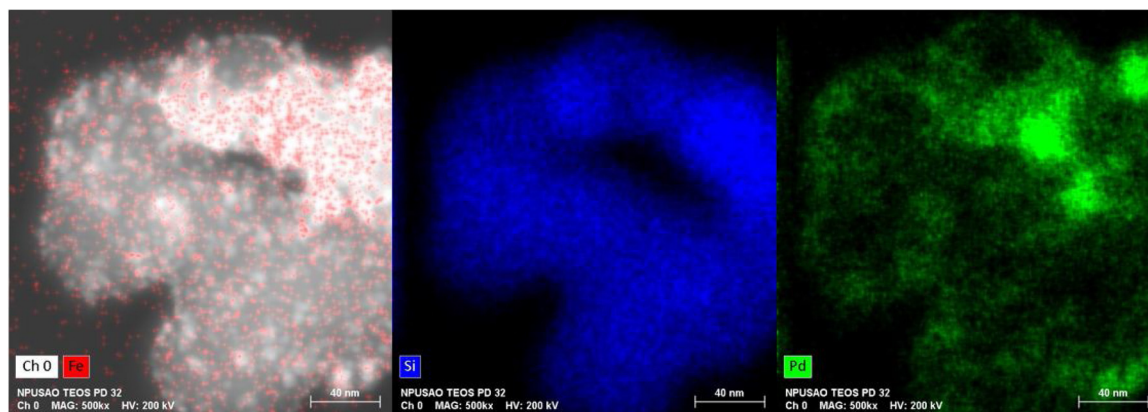


Fig. 3. Energy-dispersive X-ray spectroscopy of the MN@4.5%Pd.

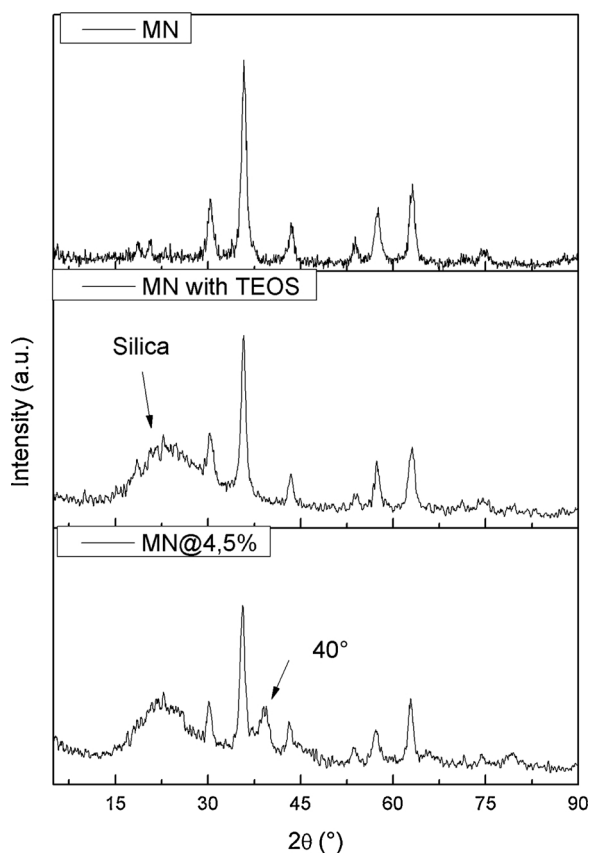


Fig. 4. XRD of MN, MN coated with TEOS and MN@4.5%Pd.

Table 1
Magnetite, Maghemite and MN XRD peaks.

Magnetite*	Maghemite*	MN
2θ (°)	2θ (°)	2θ (°)
30.10	30.28	30.35
35.43	35.69	35.80
43.06	43.35	43.50
53.41	53.87	53.90
56.96	57.42	57.35
62.53	63.03	63.10
73.97	74.56	74.25

MN synthesized in this work. *Magnetite and Maghemite peaks published by references [21,22].

the concentration of the biological catalyst on the conversion, selectivity and *ee* on the DKR of 1-phenylethylamine. It was performed by increasing the enzymatic solution during the immobilization. Results are shown on Table 3.

These optimizations could enhance considerably the amount of enzyme in the support and consequently resulted in an increase in the hydrolytic activity. The optimization 2 resulted in a hybrid catalyst with hydrolytic activity similar that found in N435, with a much lower enzyme loading. However an increasing on enzyme activity could be noted in both optimizations, it was not proportional. Nevertheless, the immobilization efficiency decreases with the successive increase of volumes, which probably shows a saturation in the number of available sites for lipase immobilization [31,32].

For palmitic acid esterification conversion, we decided to investigate the kinetic of the reaction with these catalysts, in order to obtain their initial rates, as shown in Fig. 7.

As seen before, N435 showed faster conversion an initial rates, achieving almost 77 % in the first 15 min of reaction and maximum conversion (around 80 %), after only 30 min. Compared to N435, the optimized hybrid catalysts reached a better conversion, 85 %, after 90 min, denoting lower initial rates. The esterification results did not correlate with the hydrolysis activity and with the amount of enzyme load in the support.

After obtaining and evaluating the three hybrid catalysts in the MN@4.5%Pd support, we performed the DKR of 1-phenylethylamine following reactional conditions previous published by our group [18]. Results are shown in Table 4.

Although the conversion was high for most immobilizations, the selectivity was lower and the enantiomeric excess did not improve. According to [18], the low selectivity in DKR is linked to the hydrogen source used, since in most cases the racemization is the limiting step. In the case of our hybrid catalyst, Palladium nanoparticles showed very high racemization potential. The most challenging step was to equilibrate enzyme and metal reaction times. As seen in the racemization study, once the racemic amide is obtained, its prolonged exposure to the catalyst generates by-products, decreasing the selectivity. As the enzyme is also in the reaction medium, it may react with these by-products generating more by-products. To overcome these issues and improve selectivity, ammonium formate was replaced for hydrogen gas as hydrogen donor in a new series of DKR experiments. Results are expressed on Table 5. However this modification improved the selectivity of the reaction indeed, it significantly changed the conversion results for most the immobilized biocatalysts. Comparing the results with the enzymatic load in the supports, we conclude that the best conversions were obtained by hybrid catalyst with Optimization 2.

Aiming to increase lipase CALB activity, the DKR reaction was investigated at 60 °C, since this is the best temperature applied in previous DKR reactions [33]. Results are expressed on Table 6).

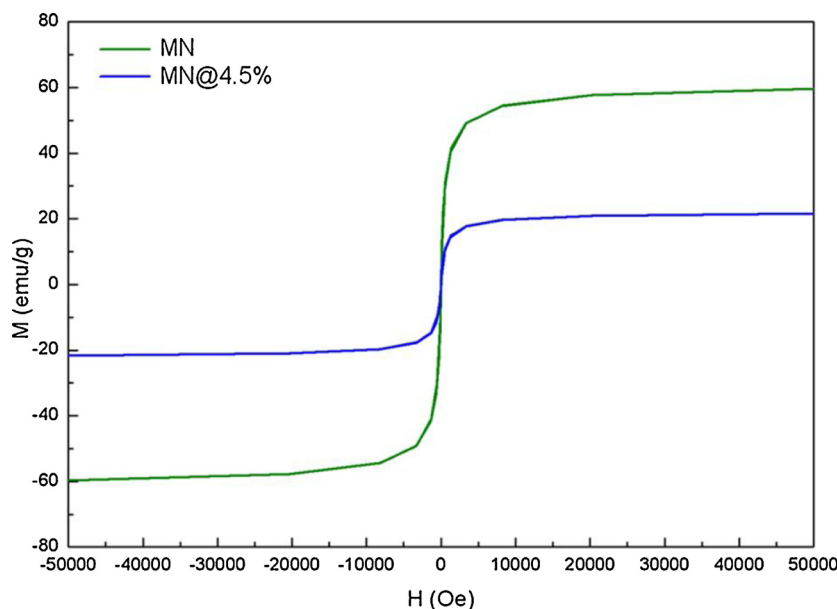


Fig. 5. Magnetization as function of the applied field.

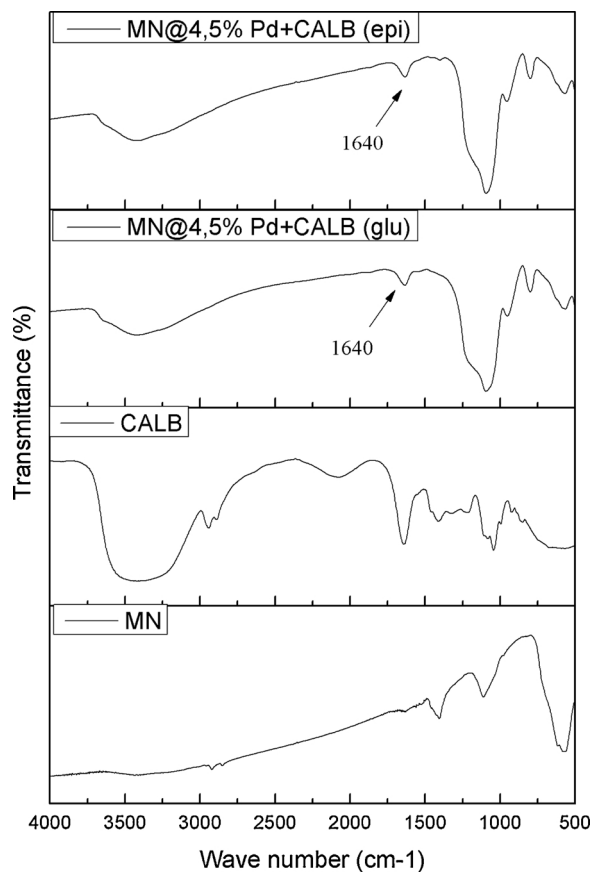


Fig. 6. Fourier transform infrared of the MN, CALB and hybrid catalysts using glutaraldehyde and epichlorohydrin.

The lower temperature contributed to the improvement of the conversion, selectivity and enantiomeric excess, and the hybrid catalysts succeeded in the DKR of (*rac*)-1-phenylethylamine. This result corroborates with the hypothesis that the enzymatic resolution was the limiting step of the DKR and that the metal catalyst is super activated.

These results were similar to the obtained by Miranda et al. commercial or non-commercial catalysts. In this work it was achieved 94 %

Table 2

Results of Immobilization of lipase CALB using glutaraldehyde and epichlorohydrin as activating agents.

Support*	Activating agent	Enzyme Loading (mg/g of support)	Hydrolytic activity (U/g)	Esterification conversion (%)		
				1 h	3 h	6 h
MN@4.5%Pd	GLU	2.96	5	63	86	84
MN@4.5%Pd	EPI	3.07	8	13	33	64
MN@	GLU	13	161	7	22	81
N435**	–	30	80	80	80	79

*MN@4.5%Pd = hybrid catalyst, MN@ = Hybrid catalyst without Pd **N435 = Novozym® 435 (commercial immobilized Lipase B de *Candida antarctica*).

of conversion and 99 % enantiomeric excess using commercial N435 and Pd/BaSO₄ at 70 °C after 12 h [18]. Xu et al. developed a palladium catalyst in MIL-101 and applied it in the reaction with N435. After 18 h, the (*R*)-amide was obtained with 99 % conversion, 93 % selectivity and > 99 % enantiomeric excess [2].

De Souza et al. develop a hybrid non-magnetic catalytic for DKR of 1-phenylethylamine and achieved 84 % conversion and > 99 % enantiomeric excess after 17 h. The constructed hybrid catalyst contained 1% palladium and 1.9 mg/g of CALB supported on silica nanoparticles [8]. Engström et al. obtained 99 % conversion with 99 % enantiomeric excess after 16 h using a hybrid catalyst containing 15.6 % palladium and 4.8 % of CALB in mesoporous silica [10].

The good results can be explained by the fact that palladium, through the applied protocol could be regularly arranged on the surface of mesoporous silica, offering a large contact surface for the racemization reaction, as well as proximity to the immobilized lipase, favoring the final DKR reaction.

The hybrid catalyst of Optimization 2 was submitted to a new series of DKR experiments under batch conditions in order to compare the metal efficiency with commercial commercial (Pd/BaSO₄) and home-made (MN@4.5 %Pd) sources of palladium, in addition to their combination with lipase N435 and CALB immobilized on magnetic particles (MN@CALB). All results were also compared with the final hybrid biocatalyst in the Table 7. As ammonium formate is a greener source of Hydrogen and easily adapted to different kinds of reactor, we decided to use the organic source of Pd.

Comparing the obtained values, it can be observed that MN@4.5 %

Table 3
Influence of the lipase amount on immobilization efficiency.

Optimization	Support mass/enzymatic solution (g/mL)	Immobilization efficiency (%)	Enzyme load (mg _{CALB} /g)	Hydrolytic activity (U/g)
Initial	1/6	76.0	2.96	5
1	1/12	50.0	3.89	10
2	1/24	35.5	5.51	63
N435	–	–	30	80

Pd as a palladium source showed lower conversions than Pd/BaSO₄ for all combinations performed. However, despite the low conversion when compared to the systems containing commercial catalysts, the values for enantiomeric excess and selectivity remained practically constant. Among the home-made catalysts, MN@4,5% Pd_{CALB} showed better results, with 74 % conversion, 90 % selectivity and enantiomeric excess > 99 % in 17 h. This result supports the hypothesis that ammonium formate can be used as a hydrogen source for chiral amine DKR [18].

Recycling

Once the best reaction conditions were determined, the recycling efficiency of the hybrid catalyst was investigated. After each cycle of DKR performed, the hybrid catalyst was washed with toluene, dried under vacuum and submitted to a new essay. In this work it was possible to perform 7 cycles of reaction as showed on Graph 1 .

As observed, the hybrid catalyst was able to maintain the conversion, selectivity and enantiomeric excess values for 4 whole DKR cycles, demonstrating robustness of both adsorbed palladium and lipase, which remain active. From the fifth cycle onwards, there was a dramatic reduction in conversion extending to the seventh cycle. Because it is a covalently bound lipase-containing biocatalyst, the risks of lipase leaching are low, as there was a strong binding between the enzyme and the support. Even so, one sample of the hybrid catalyst before the reaction and another after the reaction was submitted to Triton X-100 enzymatic desorption assay, and the residual protein was quantified by the Bradford method. As expected, no significant amounts of enzyme were detected (data not shown), demonstrating that conversion reductions are likely due to enzymatic inactivation, as the reaction takes place at 70 °C. ICP analysis (data not shown) showed that no significant amounts of palladium were found in the reaction medium, showing that it was not leached with the evolution of the recycles.

Dynamic kinetic resolution under continuous flow conditions

Considering the optimized conditions for DKR of (+/–)-α-

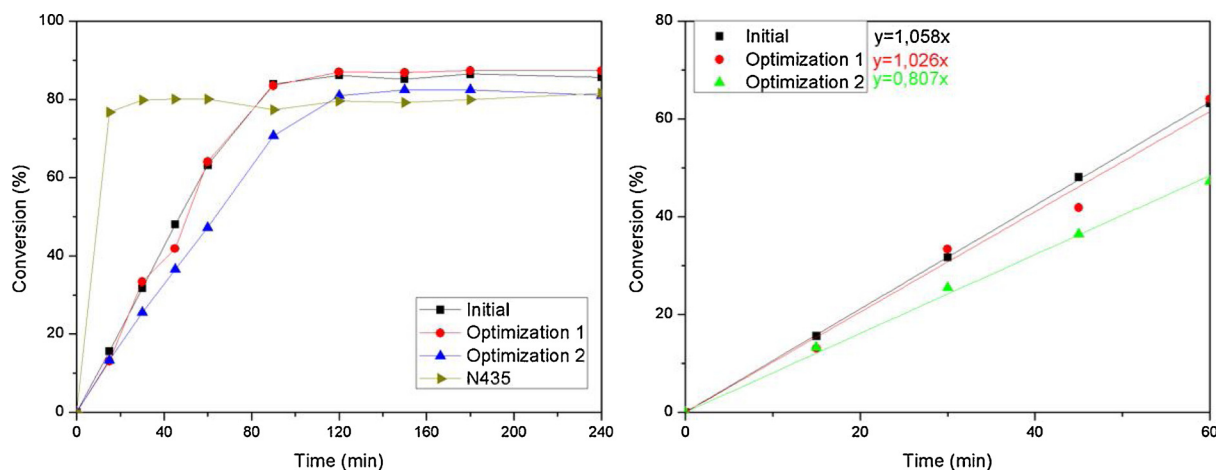


Fig. 7. Conversion and initial rates of the esterification reaction.

methylbenzylamine with the hybrid catalyst using ammonium formate as hydrogen source, the reaction was also investigated in a packed bed reactor as a way to evaluate the catalyst performance in this system, as well as reduce the reaction times.

For the supports containing only immobilized CALB, the kinetic resolution step was performed in a different compartment from the racemization reaction, allowing it to be performed at room temperature. Conversion and enantiomeric excess were monitored for up to 9 h of reaction in the looping system (figure on Table 8) and the best results obtained are presented in Table 8. For others to see supporting information.

Despite the low selectivity for MN@4.5%Pd + MN@CALB compared to MN@4.5%Pd + N435 (Entries 1 and 2) there was a decrease in reaction time from 4 to 1 h. In addition, the conversion values were higher than those obtained using the commercial catalyst with the palladium source, with a small difference in selectivity and without significantly affecting the enantiomeric excess of the product (Entries 3-4).

For catalyst MN@4.5%Pd_{CALB} (Entry 5) no increase in total reaction time conversion was observed, but selectivity and enantiomeric excess did not change significantly over time (see supporting information). The low conversion observed may be related to the conditions of the reaction medium, which favors the palladium racemization stage that has a high activity, however, the high temperature required may end up compromising the lipase resolution stage, reflecting in the lower conversion results. Presented [33]. Unlike the batch reaction, in the continuous flow system the product formed is less exposed to the catalyst, which may justify the small changes in selectivity.

Conclusion

The magnetic hybrid catalyst showed a very good performance in the DKR of (*rac*)-1-phenylethylamine with four regular recycles without significant loss in conversion, selectivity and enantiomeric excess. Similar results in conversion and selectivity were found if compared to commercial catalytic systems (N435 and Pd/BaSO₄), and higher to the ones obtained with previous biocatalysts in a lower reaction

Table 4
DKR of optimized hybrid catalysts MN@4.5%Pd using ammonium formate and at 70 °C [18].

Immob	Conversion (%)	Selectivity (%)	ee _p (%)
Initial	88	75	86
Optimization 1	89	55	87
Optimization 2	94	63	86

*MN@4.5%PdGLU = hybrid catalyst with 4.5 % of palladium using glutaraldehyde.

temperature.

The characterization showed that the support used in the hybrid catalyst is composed by magnetite or maghemite, is nanometric, superparamagnetic and that the palladium nanoparticles are supported in the silica-coating surface. The saturation magnetization was reduced when the silica was coated on the surface, however, it was still possible to separate it using a magnetic field.

Experimental section

Pd- nanomagnetic particles(@MNPd) preparation

Iron oxide nanoparticles were synthesized according to [22]. 0.02 mol of FeSO₄·7H₂O and 0.04 mol FeCl₃ were dissolved in 40 mL of distilled water and heated to 80 °C for 1 h with magnetic stirring. 5 mL of an acetone solution containing 0.1 mL of oleic acid was added. A stoichiometric amount of NH₄OH was added and the sample was sonicated for 15 min, followed by washing with acetone and methanol (1:1) solution at room temperature. 2 g of iron oxides were sonicated in 300 mL of ethanol and 25 mL of water, 9 mL of NH₄OH were added and stirred at 700 rpm for 10 min. Then, 45 mL of TEOS were added and the medium was stirred for 3 h at 40 °C and 21 h at room temperature. The silica coated nanoparticles were recovered with a magnet and washed with ethanol. Then, 2.25 mL of APTES were added and the medium was stirred at 700 rpm for 16 h. The nanoparticles were recovered with a magnet and washed with ethanol.

In a different reactor, 0.15 M solution of H₂PdCl₄ was prepared with HCl and PdCl₂ in a aqueous solution at 50 °C for 30 min, followed by addition of 500 mg of the nanoparticles previous prepared. Then, 400 μL of a 10 % NaBH₄ solution was added and the medium was homogenized for 10 min. 2 mL of NH₄OH was added and the medium was stirred for 1 h. The nanoparticles were recovered with a magnet and washed with ethanol and dried under vacuum.

Table 5
DKR of MN@4.5%Pd using H₂ and at 70 °C [18].

Immobilization	Conversion (%)	Selectivity (%)	ee _p (%)
Initial	61	72	85
1	87	94	86
2	> 99	94	91

*MN@4.5%PdGLU = Magnetic nanoparticles with 4.5 % of palladium using glutaraldehyde.

Racemization reactions

Racemization of (S)-1-phenylethylamine was conducted according to [18]. In 4 mL vial, 3 mL of dried toluene, 0.1 M of (S)-1-phenylethylamine, 1.5 equivalents of ammonium formate, 12 mg Na₂CO₃ and 375 mg of molecular sieves were added. The reaction was kept at 70 °C under inert atmosphere and the amount of MN added varied according to the Pd concentration in each, in order to have 30 mol% of palladium. Samples were derivatized with 5 μL of trifluoroacetic anhydride and 5 μL of triethylamine and analyzed on a Shimadzu GC-2010 gas chromatograph with flame ionization detector and CP-Chirasil-Dex CB (25 m X0.25 mm ID) chiral column using hydrogen as carrier gas. Injector and detector temperatures were set at 220 °C. The column started at 90 °C and held for 15 min before it was heated to 190 °C at 40 °C/min and held at that temperature for 5 min. Biphenyl was used as internal standard for racemization reactions and conversion, selectivity and enantiomeric excess were calculated according to the equations below.

$$\text{Conversion (\%)} = 100 - \frac{A_{S_n}/A_{B_n}}{A_{S_0}/A_{B_0}} \times 100$$

$$\text{Selectivity (\%)} = 100 - \frac{A_{Sub_n}}{A_{S_n} + A_{R_n} + A_{Sub_n}} \times 100$$

$$ee (\%) = \left(\frac{A_{S_n}}{A_{S_n} + A_{R_n}} - \frac{A_{R_n}}{A_{S_n} + A_{R_n}} \right) \times 100$$

Where, is the area corresponding to (S)-1-phenylethylamine before the reaction, is the area of biphenyl before the reaction and A_{S_n}, A_{R_n}, A_{B_n}, A_{sub_n} are the areas of (S)-1-phenylethylamine, (R)-1-phenylethylamine, biphenyl and byproducts at the appropriate time.

Lipase immobilization

Lipase immobilization by covalent bond were performed according to [34]: 500 mg of covered @MNPd were dispersed in 10 mL of a phosphate buffer (pH7 and 50 mM) containing 2 mL of glutaraldehyde

Table 6
DKR of MN@4.5%Pd using H₂ and at 60 °C.

Immobilization	Conversion (%)	Selectivity (%)	ee _p (%)
Initial	78	96	95
1	90	97	95
2	> 99	95	92

*MN@4.5%PdGLU = Magnetic nanoparticles with 4.5 % of palladium using glutaraldehyde.

during 24 h. After washing with distilled water, 1 mL of CALB diluted in 5 mL of phosphate buffer (pH 7 and 25 mM) were added to 1 g of support and the immobilization was done in shaker at 40 °C and 150 rpm for 24 h.

Immobilization using epichlorohydrin was done according to [35]. 1 g of the support was activated in a shaker for 1 h at 120 rpm and 25 °C with 10 mL solution of epichlorohydrin (2.5 %) in phosphate buffer (pH 7.5 and 0.1 M). The support was recovered with magnetic separation and washed with distilled water. Then, the support was soaked with 10 mL of hexane and stirred at 120 rpm for 2 h at 25 °C. Excess of hexane was removed and 1 mL of CALB diluted in 5 mL of phosphate buffer (pH 7 and 25 mM) was added to the support. The immobilization was conducted at 4 °C for 16 h followed by washing with hexane. Immobilization efficiency in both biocatalysts was evaluated by Bradford method [28].

Hydrolytic activity

The hydrolytic activity was made by the titration method with olive oil, according to the protocol of [36], being an unit of enzyme activity (U) defined as the amount of enzyme in grams used to release 1 μmol of fatty acid per minute under the experimental conditions. An emulsion containing 5 % of extra virgin olive oil and 5 % of arabic gum was prepared in a phosphate buffer (pH 7 and 100 mM) and 20 mL of this emulsion was added to 10 mg of the biocatalyst. The reaction was incubated at 37 °C for 30 min and the reaction was stopped with 20 mL of an acetone and ethanol solution (1:1). The titration of the fatty acids produced was done using a 0.04 M NaOH until pH 11 using a Mettler Toledo automatic titrator. Control samples were made under the same conditions without the incubation of the catalyst.

Table 7
DKR of catalyst using ammonium formate and at 70 °C in batch condition.

Catalyst*	Conversion (%)	Selectivity (%)	ee _p (%)
MN@4.5%Pd + MN@CALB	56	89	98
MN@4.5%Pd + N435	60	87	98
Pd/BaSO ₄ + MN@CALB	71	89	> 99
Pd/BaSO ₄ + N435	> 99	94	> 99
MN@4.5%Pd_CALB	74	90	> 99

*MN@4.5%Pd = Magnetic nanoparticle with 4.5 % palladium, MN@ = hybrid catalyst without enzyme; **N435 = Novozym® 435 (Lipase B de *Candida antarctica* immobilized) commercial; Pd/BaSO₄ = Palladium immobilized on Barium Sulphate (Commercial) MN@4.5%Pd_CALB = optimized hybrid catalyst.

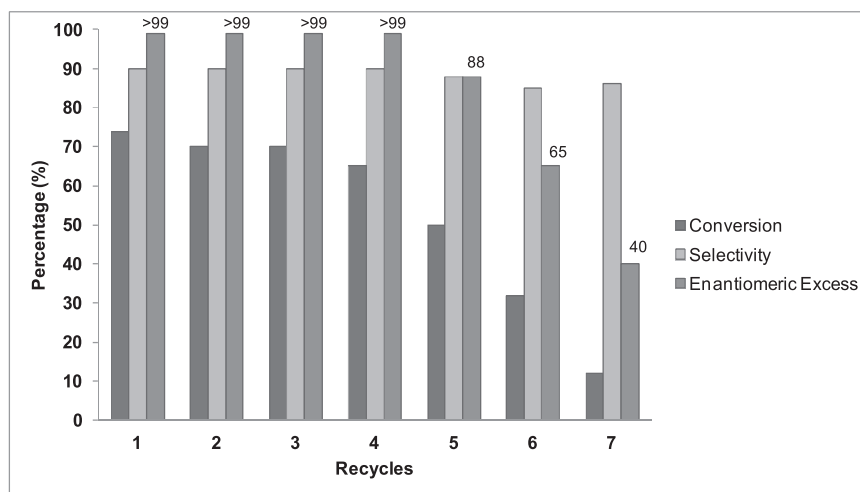
Esterification potential

The esterification potential was done with palmitic acid and ethanol according to [34]. In a 4 mL vial, a solution containing 100 mM of palmitic acid, 100 mM ethanol in heptane was added together with 30 mg of the biocatalyst. The reaction was conducted at 50 °C and the aliquots were derivatized with M-methyl-N-9-trimethylsilyl) trifluoroacetamide and analyzed on a Shimadzu GC-2010 gas chromatograph with flame ionization detector and HP-5MS column using hydrogen as carrier gas. Injector and detector temperatures were set at 250 °C. The column started at 100 °C and held for 1 min before it was heated to 180 °C at 15 °C/min and held at that temperature for 1 min. The conversion was calculated according to the equation below, where A_{aci} is the area of the palmitic acid and A_{est} is the area of the produced ester. A calibration curve was done with the palmitic acid.

$$\text{Conversion (\%)} = 100 - \frac{A_{aci}}{A_{aci} + A_{est}} * 100$$

Dynamic kinetic resolution

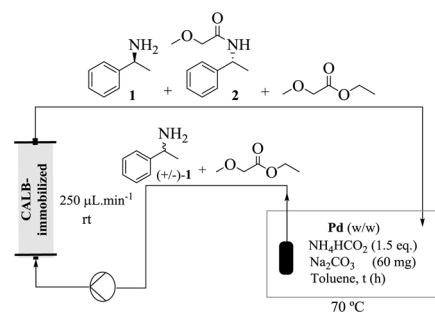
The dynamic kinetic resolution of (rac)-1-phenylethylamine was conducted according to [18]. In 4 mL vial, 3 mL of previously dried and distilled toluene, 200 mg of the hybrid catalyst, 0.1 M of (S)-1-phenylethylamine, 0.2 M methyl 2-methoxyacetate, 12 mg Na₂CO₃ and 375 mg of molecular sieves were added. As hydrogen donor, H₂ gas or 1.5 equivalents of ammonium formate were used (in this case, a bubbler was coupled to the vial to reduce the pressure of the medium). 100 μL samples were analyzed on a Shimadzu GC-2010 gas chromatograph with flame ionization detector and CP-Chirasil-Dex CB (25 m X0.25 mm ID) chiral column using the same methodology as the one described for racemization. Conversion, selectivity and enantiomeric excess were



Graph 1. Recycles of hybrid catalyst on DKR of (+/−)-α-methylbenzylamine in batch conditions using ammonium formate under batch conditions.

Table 8

DKR of catalyst using ammonium formate in continuous flow condition.



Entry	Catalyst (Pd + CALB-immob.)	Reaction Time (h)	Conversion (%)	Selectivity (%)	ee _p (%)
1	MN@4.5%Pd + MN@CALB	1	95	71	> 99
2	MN@4.5%Pd + N435	4	> 99	96	> 99
3	Pd/BaSO ₄ + MN@CALB	1	65	84	> 99
4	Pd/BaSO ₄ + N435	1	72	94	97
5	MN@4.5%Pd_CALB*	9	65	88	> 99

*MN@4.5%Pd = Magnetic nanoparticle with 4.5 % palladium, MN@ = hybrid catalyst without enzyme; **N435 = Novozym® 435 (Lipase B de *Candida antarctica* immobilized) commercial; Pd/BaSO₄ = Palladium immobilized on Barium Sulphate (Commercial) MN@4.5%Pd_CALB = optimized hybrid catalyst.

calculated according to the equations below.

$$\text{Conversion (\%)} = \frac{A_{PR} + A_{PS} + A_{By}}{A_S + A_{PR} + A_{PS} + A_{By}}$$

$$\text{Selectivity (\%)} = 100 - \frac{A_{By}}{A_{PR} + A_{PS} + A_{By}} * 100$$

$$ee_p = \left(\frac{A_{PR}}{A_{PR} + A_{PS}} - \frac{A_{PS}}{A_{PR} + A_{PS}} \right) \times 100$$

Where, A_{PR} is the area of the (R)-2-methoxy-N-(1-phenylethyl) acetamide, A_{PS} is the area of the (S)-2-methoxy-N-(1-phenylethyl) acetamide, A_S is the area of the substrate, and A_{By} is the area of the byproducts.

Hybrid catalyst recycles

The hybrid catalysts were separated with a magnet after the racemization and the kinetic resolution and washed 4 times with 2 mL of toluene. They were dried overnight and applied again in the same reaction conditions.

Dynamic resolution under continuous flow conditions

A stock solution containing 3.2 mmol of *rac*-(α-Methylbenzylamine) and methyl 2-methoxyacetate (6.4 mmol) in toluene was transferred into an Erlenmeyer flask containing Pd/BaSO₄ (0.48 mmol of Pd), Na₂CO₃ (60 mg) and molecular sieves at room temperature and connected to a packed-bed reactor (2.35 cm³) filled with immobilized CALB (900 mg). The solution was pumped through the reactor at a rate of 250 μL.min⁻¹ (residence time of 9.4 min) at room temperature. Ammonium formate (150 mg, 1.6 mmol) was added to flask which was heated to 70 °C while the reactor was filled with immobilized CALB at room temperature. When hybrid catalyst was applied, sodium carbonate and ammonium formate were packaged together with the catalyst and kept at 70 °C during reaction. The solution was circulated through system until 9 h. Samples were collected and Enantiomeric excesses were determined by GC equipped with a chiral column. A GC-MS was used to identify byproducts and as well as the relative amount of (+/−)-(α-Methylbenzylamine, 2-methoxy-N-(1-phenylethyl)acetamide and reaction byproducts.

Characterizations

- Fourier-transform infrared (FTIR) spectroscopy: KBr pellets were prepared for the evaluation in a Nicolet Magna FTIR-760 equipment in the range of 4000–400 cm⁻¹.
- X-ray diffraction: The analysis were performed in the Laboratory of Hydrogen Technology of the School of Chemistry, Federal University of Rio de Janeiro in a Rigaku Mminiflex II diffractometer with copper anode (Cu K α , 30 kV and 15 mA) with 0.05° step and 1 s per step in the range of 5–90°. The diameter of the crystallites were estimated using Scherrer's equation as a function of the highest intensity peak [37], where D_c is the diameter in nm, k the proportionality constant (0.94 for spherical particles), λ the wavelength of the radiation (0.1542 nm for Cu K α), θ the angle of the highest peak, and β the width at half height of the peak.

$$D_c = \frac{k \lambda}{\beta \cos(\theta)}$$

- Transmission electron microscopy: 10 mg of the samples were sonicated in 10 mL of distilled water for 5 min. The images were made in a JEOL 2100 F 200 kV microscope and a Noran Seven energy-dispersive X-ray spectroscopy system.
- Magnetometry: The essay was conducted in a Quantum Design PPMS Dynacool equipment equipped with a vibrating sample magnetometer at 300 K in the range of –50,000 to 50,000 Oe.

Declaration of Competing Interest

The authors declare that they have no known competing financial interests or personal relationships that could have appeared to influence the work reported in this paper.

CRediT authorship contribution statement

Clara A. Ferraz: Conceptualization, Formal analysis, Investigation. **Marcelo A. do Nascimento:** Data curation, Formal analysis, Writing - original draft. **Rhudson F.O. Almeida:** Methodology, Formal analysis. **Gabriella G. Sergio:** Methodology. **Aldo A.T. Junior:** Validation, Formal analysis, Methodology. **Gisele Dalmônico:** Formal analysis, Data curation. **Richard Caraballo:** Data curation. **Priscilla V. Finotelli:** Validation, Data curation, Writing - original draft. **Raquel A.C. Leão:** Data curation, Writing - review & editing. **Robert Wojcieszak:** Funding acquisition, Writing - original draft, Resources. **Rodrigo O.M.A. de Souza:** Conceptualization, Funding acquisition, Project administration, Resources, Supervision, Writing - original draft, Writing - review & editing. **Ivaldo Itabaiana:** Conceptualization, Funding acquisition, Project administration, Resources, Supervision, Writing - original draft, Writing - review & editing.

Acknowledgements

Authors thank CAPES, CNPq and FAPERJ for financial support. LIA CNRS France-Brazil “Energy & Environment” and CatBioInnov FEDER (LS197801) are also acknowledged.

Chevreul Institute (FR 2638), Ministère de l'Enseignement Supérieur, de la Recherche et de l'Innovation, Région Hauts-de-France, Métropole Européenne de Lille, and FEDER are acknowledged for supporting and funding partially this work. This study was supported by the French government through the Programme Investissement d'Avenir (I-SITE ULNE / ANR-16-IDEX-0004 ULNE) managed by the Agence Nationale de la Recherche.

Appendix A. Supplementary data

Supplementary material related to this article can be found, in the online version, at doi:<https://doi.org/10.1016/j.mcat.2020.111106>.

References

- [1] D. Ghislieri, N.J. Turner, Biocatalytic approaches to the synthesis of enantiomerically pure chiral amines, *Top. Catal.* 57 (2014) 284–300, <https://doi.org/10.1007/s11244-013-0184-1>.
- [2] S. Xu, M. Wang, B. Feng, X. Han, Z. Lan, H. Gu, H. Li, H. Li, Dynamic kinetic resolution of amines by using palladium nanoparticles confined inside the cages of amine-modified MIL-101 and lipase, *J. Catal.* 363 (2018) 9–17, <https://doi.org/10.1016/j.jcat.2018.04.006>.
- [3] A. Schmid, J.S. Dordick, B. Hauer, A. Kiener, M. Wubbolt, B. Witholt, *Industrial biocatalysis and tomorrow*, *Nature* 409 (2001) 258–268.
- [4] D. Muñoz Solano, P. Hoyos, M.J. Hernáiz, A.R. Alcántara, J.M. Sánchez-Montero, Industrial biotransformations in the synthesis of building blocks leading to antiopiure drugs, *Bioresour. Technol.* 115 (2012) 196–207, <https://doi.org/10.1016/j.biortech.2011.11.131>.
- [5] A.S. De Miranda, L.S.M. Miranda, R.O.M.A. De Souza, Lipases: valuable catalysts for dynamic kinetic resolutions, *Biotechnol. Adv.* (2015), <https://doi.org/10.1016/j.biotechadv.2015.02.015>.
- [6] Z.S. Seddigi, M.S. Malik, S.A. Ahmed, A.O. Babalghith, A. Kamal, Lipases in asymmetric transformations: recent advances in classical kinetic resolution and lipase–metal combinations for dynamic processes, *Coord. Chem. Rev.* 348 (2017) 54–70, <https://doi.org/10.1016/j.ccr.2017.08.008>.
- [7] O. Långvik, T. Saloranta, D.Y. Murzin, R. Leino, Heterogeneous chemoenzymatic catalyst combinations for one-pot dynamic kinetic resolution applications, *ChemCatChem* 7 (2015) 4004–4015, <https://doi.org/10.1002/cctc.201500459>.
- [8] S.P. de Souza, R.A.C. Leão, J.F. Bassut, I.C.R. Leal, S. Wang, Q. Ding, Y. Li, F.L.Y. Lam, R.O.M.A. de Souza, I. Itabaiana, New Biosilified Pd-lipase hybrid biocatalysts for dynamic resolution of amines, *Tetrahedron Lett.* 58 (2017) 4849–4854, <https://doi.org/10.1016/j.tetlet.2017.11.031>.
- [9] (a) A.K. Ganai, P. Shinde, B.B. Dhar, S. Sen Gupta, B.L.V. Prasad, Development of a multifunctional catalyst for a “relay” reaction, *RSC Adv.* 3 (2013) 2186–2191, <https://doi.org/10.1039/c2ra22829g>;
(b) O. Verho, J.-E. Bäckvall, *Am. Chem. Soc.* 137 (12) (2015) 3996–4009, <https://doi.org/10.1021/jacs.5b01031>.
- [10] (a) K. Engström, E.V. Johnston, O. Verho, K.P.J. Gustafson, M. Shakeri, C.W. Tai, J.E. Bäckvall, Co-immobilization of an enzyme and a metal into the compartments of mesoporous silica for cooperative tandem catalysis: an artificial metalloenzyme, *Angew. Chemie - Int. Ed.* 52 (2013) 14006–14010, <https://doi.org/10.1002/anie.201306487>;
(b) X. Li, Y. Cao, K. Luo, Y. Sun, J. Xiong, L. Wang, Z. Liu, J. Li, J. Ma, J. Ge, H. Xiao, R.N. Zare, Highly active enzyme–metal nanohybrids synthesized in protein–polymer conjugates, *Nat. Catal.* 2 (2019) 718–725.
- [11] A. Pellis, S. Cantone, C. Ebert, L. Gardossi, Evolving biocatalysis to meet bioeconomy challenges and opportunities, *N. Biotechnol.* 40 (2018) 154–169, <https://doi.org/10.1016/j.nbt.2017.07.005>.
- [12] C.W. Lim, I.S. Lee, Magnetically recyclable nanocatalyst systems for the organic reactions, *Nano Today* 5 (2010) 412–434, <https://doi.org/10.1016/j.nantod.2010.08.008>.
- [13] Z.Y. Ma, X.Q. Liu, Y.P. Guan, H.Z. Liu, Synthesis of magnetic silica nanospheres with metal ligands and application in affinity separation of proteins, *Colloids Surfaces A Physicochem. Eng. Asp.* 275 (2006) 87–91, <https://doi.org/10.1016/j.colsurfa.2005.04.045>.
- [14] L.M. Rossi, Recent Advances in the Development of Magnetically Recoverable Metal Nanoparticle Catalysts, (2012), <https://doi.org/10.1590/S0103-50532012001100002>.
- [15] S.A. Ansari, Q. Husain, Potential applications of enzymes immobilized on/in nano materials: a review, *Biotechnol. Adv.* 30 (2012) 512–523, <https://doi.org/10.1016/j.biotechadv.2011.09.005>.
- [16] M. Bilal, Y. Zhao, T. Rasheed, H.M.N. Iqbal, Magnetic nanoparticles as versatile carriers for enzymes immobilization: a review, *Int. J. Biol. Macromol.* 120 (2018) 2530–2544, <https://doi.org/10.1016/j.ijbiomac.2018.09.025>.
- [17] M. Shakeri, C. Tai, E. Gthelid, S. Oscarsson, Small Pd Nanoparticles Supported in Large Pores of Mesocellular Foam: An Excellent Catalyst for Racemization of Amines, (2011), pp. 13269–13273, <https://doi.org/10.1002/chem.201101265>.
- [18] A.S. De Miranda, R.O.M.A. De Souza, L.S.M. Miranda, Ammonium formate as a green hydrogen source for clean semi-continuous enzymatic dynamic kinetic resolution of (+/-)- α -methylbenzylamine, *RSC Adv.* 4 (2014) 13620–13625, <https://doi.org/10.1039/c4ra00462k>.
- [19] L.L. Chng, N. Erathodiyil, J.Y. Ying, Nanostructured Catalysts for Organic Transformations, XXX (2012).
- [20] D.K. Yi, S.S. Lee, J.Y. Ying, Synthesis and Applications of Magnetic Nanocomposite Catalysts 18 (2006), pp. 2004–2006.
- [21] M.Z. Kassaee, H. Masroufi, F. Movahedi, Applied Catalysis A: general sulfamic acid-functionalized magnetic Fe 3 O 4 nanoparticles as an efficient and reusable catalyst for one-pot synthesis of α -amino nitriles in water, *Appl. Catal. A, Gen.* 395 (2011) 28–33, <https://doi.org/10.1016/j.apcata.2011.01.018>.
- [22] D. Maity, D.C. Agrawal, Synthesis of iron oxide nanoparticles under oxidizing environment and their stabilization in aqueous and non-aqueous media, *J. Magn. Magn. Mater.* 308 (2007) 46–55, <https://doi.org/10.1016/j.jmmm.2006.05.001>.

- [23] E.S.D.T. de Mendonça, A.C.B. de Faria, S.C.L. Dias, F.F.H. Aragón, J.C. Mantilla, J.A.H. Coaquira, J.A. Dias, Effects of Silica Coating on the Magnetic Properties of Magnetite Nanoparticles, (2018), <https://doi.org/10.1016/J.SURFIN.2018.11.005>.
- [24] Y. Hammiche-Bellal, A. Benadda-Kordjani, R. Benrabaa, A. Djadoun, L. Meddour-Boukhobza, Efficiency of magnetite as nanocrystalline bulk catalyst for the reduction of 4-nitrophenol, *J. Environ. Chem. Eng.* 6 (2018) 2355–2362, <https://doi.org/10.1016/j.jece.2018.03.042>.
- [25] M. Ganesan, R.G. Freemantle, S.O. Obare, Monodisperse thioether-stabilized palladium nanoparticles: synthesis, characterization, and reactivity, *Chem. Mater.* 19 (2007) 3464–3471, <https://doi.org/10.1021/CM062655Q>.
- [26] S.J. Schön, *Magnetic Properties* 65 (2011), pp. 373–391, [https://doi.org/10.1016/S1567-8032\(11\)08010-4](https://doi.org/10.1016/S1567-8032(11)08010-4).
- [27] B. Thangaraj, Z. Jia, L. Dai, D. Liu, W. Du, Effect of silica coating on Fe₃O₄ magnetic nanoparticles for lipase immobilization and their application for biodiesel production, *Arab. J. Chem.* (2016), <https://doi.org/10.1016/j.arabjc.2016.09.004>.
- [28] M.M. Bradford, A rapid and sensitive method for the quantitation of microgram quantities of protein utilizing the principle of protein-dye binding, *Anal. Biochem.* 254 (1976) 248–254, [https://doi.org/10.1016/0003-2697\(76\)90527-3](https://doi.org/10.1016/0003-2697(76)90527-3).
- [29] G. Chen, C. Kuo, C. Chen, C. Yu, C. Shieh, Y. Liu, Effect of membranes with various hydrophobic / hydrophilic properties on lipase immobilized activity and stability, *JBIOSEC* 113 (2012) 166–172, <https://doi.org/10.1016/j.jbiosc.2011.09.023>.
- [30] R.C. Rodrigues, C. Ortiz, A. Berenguer-Murcia, R. Torres, R. Fernández-Lafuente, Modifying enzyme activity and selectivity by immobilization, *Chem. Soc. Rev.* 42 (2013) 6290–6307, <https://doi.org/10.1039/c2cs35231a>.
- [31] D.S. Rodrigues, A.A. Mendes, W.S. Adriano, L.R.B. Gonc, R.L.C. Giordano, Multipoint covalent immobilization of microbial lipase on chitosan and agarose activated by different methods, *J. Mol. Catal., B Enzym.* 51 (2008) 100–109, <https://doi.org/10.1016/j.molcatb.2007.11.016>.
- [32] D. Zhang, L. Peng, Y. Wang, Y. Li, Lipase immobilization on epoxy-activated poly (vinyl acetate-acrylamide) microspheres, *Colloids Surf. B Biointerfaces* 129 (2015) 206–210, <https://doi.org/10.1016/j.colsurfb.2015.03.056>.
- [33] U. Jonas, T.H. Mogens, P. Shamkant, J. Alwyn, The sequence, crystal structure determination and refinement of two crystal forms of lipase B from *Candida antarctica*, *Structure* 2 (1994) 293–308, [https://doi.org/10.1016/S0969-2126\(00\)00031-9](https://doi.org/10.1016/S0969-2126(00)00031-9).
- [34] S.P. de Souza, I.I. Junior, G.M.A. Silva, L.S.M. Miranda, M.F. Santiago, F.L. Lam, A. Dawood, U.T. Bornscheuer, R.O.M.A. De Souza, Cellulose as an efficient matrix for lipase and transaminase immobilization, *RSC Adv.* 6 (2016) 6665–6671, <https://doi.org/10.1039/c5ra24976g>.
- [35] L.S. Martin, A. Ceron, P.C. Oliveira, G.M. Zanin, H.F. de Castro, Different organic components on silica hybrid matrices modulate the lipase inhibition by the glycerol formed in continuous transesterification reactions, *J. Ind. Eng. Chem.* 62 (2018) 462–470, <https://doi.org/10.1016/j.jiec.2018.01.029>.
- [36] D.M. Freire, E.M.F. Teles, E.P.S. Bon, G.L.S. Anna, Lipase production by *Penicillium restrictum* in a bench-scale fermenter, *Appl. Biochem. Biotechnol.* 63–65 (1997) 409–421, <https://doi.org/10.1007/BF02920442>.
- [37] A.L. Patterson, The scherrer formula for X-ray particle size determination, *Phys. Rev.* 56 (1939) 978–982, <https://doi.org/10.1103/PhysRev.56.978>.